



PCCP

**Effects of Electrostatic Drag on the Velocity of Hydrogen Migration – Pre- and Post-Transition State Enthalpy/Entropy Compensation**

Journal:	<i>Physical Chemistry Chemical Physics</i>
Manuscript ID	CP-ART-09-2020-005000.R2
Article Type:	Paper
Date Submitted by the Author:	06-Nov-2020
Complete List of Authors:	Xing, Yang-Yang; Shandong Normal University, College of Chemistry, Chemical Engineering and Materials Science Chen, Shusen; University of California, Davis, Chemistry Chen, Dezhan; Shandong Normal University, College of Chemistry, Chemical Engineering and Materials Science Tantillo, Dean; University of California, Davis, Chemistry;

SCHOLARONE™  
Manuscripts

## Effects of Electrostatic Drag on the Velocity of Hydrogen Migration – Pre- and Post-Transition State Enthalpy/Entropy Compensation

Yang-Yang Xing,<sup>†,‡</sup> Shu-Sen Chen<sup>‡</sup>, De-Zhan Chen<sup>†</sup> and Dean J. Tantillo<sup>\*,‡</sup>

<sup>†</sup>College of Chemistry, Chemical Engineering and Materials Science, Collaborative Innovation Center of Functionalized Probes for Chemical Imaging in Universities of Shandong, Shandong Normal University, Jinan 250014, P. R. China

<sup>‡</sup>Department of Chemistry, University of California, Davis, California 95616, United States

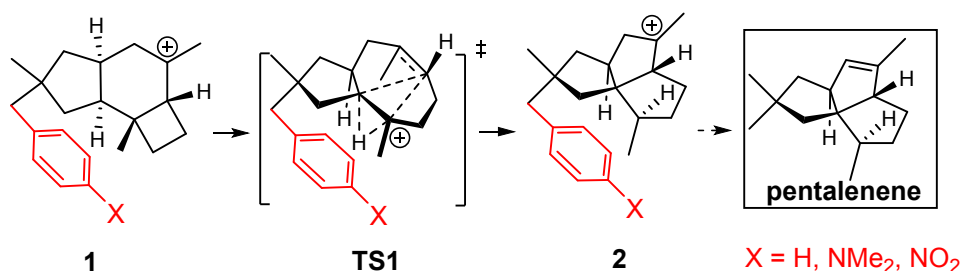
### Abstract

Ab initio molecular dynamics calculations were used to explore the underlying factors that modulate the velocity of hydrogen migration for 1,2 hydrogen shifts in carbocations in which different groups interact noncovalently with the migrating hydrogen. Our results indicate that stronger electrostatic interactions between the migrating hydrogen and nearby  $\pi$ -systems lead to slower hydrogen migration, an effect tied to entropic contributions from the hydrogen + neighboring group substructures.

### 1. Introduction

The carbocation cyclization/rearrangement process that leads to the complex sesquiterpene pentalenene has served as a testing ground for many mechanistic concepts.<sup>1</sup> In 2006, it was proposed that the dyotropic rearrangement<sup>2</sup> shown in Scheme 1 (without the covalently attached aryl group) might be promoted by a through-space interaction between an enzymatic aryl group and the migrating hydrogen, the latter of which bears positive charge.<sup>1a,3</sup> In 2014, computational results for the specific systems shown in Scheme 1 were described, systems designed to convert the previously proposed intermolecular interaction into an intramolecular one.<sup>1b</sup> These results indicated that the barrier for rearrangement was lower with a  $\pi$ -donating substituent on the aryl group and higher with a  $\pi$ -accepting group (compared to the X = H system).

We now reexamine these systems to assess the effects of such interactions on the *momentum of the migrating groups*. In 2017, based on the results of direct dynamics simulations on a different carbocation rearrangement, we argued for the potential importance of a phenomenon we called “electrostatic drag”, i.e., the slowing down of a migrating group due to favorable through-space electrostatic interactions.<sup>4</sup> Here we provide an initial assessment of the generality of this concept and connect it to the concept of enthalpy/entropy compensation.<sup>5</sup> While the dyotropic rearrangement we examine has been shown to be unlikely in a biological setting,<sup>1c</sup> it provides a convenient framework for further exploring the electrostatic drag concept.



Scheme 1. Dyotropic rearrangement for conversion of carbocations **1** to carbocations **2**, the latter of which sport pentalenene frameworks.

## 2. Computational Methods

Geometry optimizations were performed using Gaussian 09<sup>6</sup> at the B3LYP<sup>7</sup>/6-31+G(d,p) level in the gas phase. Gaussrate 17<sup>8</sup> and Polyrate 17<sup>9</sup> were used to find variational transition states (VTSS). Intrinsic reaction coordinate (IRC) calculations<sup>10</sup> were performed to confirm connections between key transition-state structures (TSSs) and corresponding reactants and products on potential energy surfaces (PES). Singleton's Progdyn script package<sup>11</sup> was used to conduct quasi-classical on-the-fly ab initio molecular dynamics simulations,<sup>12</sup> which were initialized starting from regions of PES TSSs. The following geometric stop criteria were used to determine the outcome of each trajectory (atom numbers shown in Figure 1): In the reverse direction, we labeled a trajectory as forming the reactant when the H1-C1-C2 angle reached 90°. In the forward direction, we labeled a trajectory as forming the product when the C1-C2-H1 angle reached 90°. We discuss velocity below from the perspective of times taken to complete trajectories (based on trajectory endpoints, irrespective of distances traveled). We quantified hydrogen migration velocities using distances traveled by hydrogen atoms as well (distance/time; see Tables S1 and S2), and results agreed with those based on trajectory time. Trajectories for **TS-N(CH<sub>3</sub>)<sub>2</sub>**, **TS-H** and **TS-NO<sub>2</sub>** were also obtained using B3LYP-D3<sup>13a,b</sup> and M06-2X<sup>13b,c</sup> to account for effects of dispersion. Tunneling is not considered here (see Supporting Information for test calculations on tunneling corrections). While counterion effects are likely to be significant, here we quantify reactivity in the absence of counterions to reveal the effects originating in the substrate; similar approaches have been used in many previous studies of carbocation reactions.<sup>14</sup> The 3D structures shown were illustrated using CYLview.<sup>15</sup> The CHelpG electrostatics-based model was employed to compute partial atomic charges.<sup>16</sup>

## 3. Results and Discussion

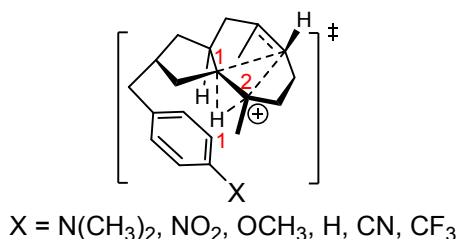


Figure 1. Aromatic groups used to explore the hydrogen migration process.

Initially, a series of substituents on the aryl group of **1** was employed to quantify effects of through-space cation– $\pi$  interactions on the velocity of hydrogen migration (Figure 1). Average whole time (from B3LYP/6-31+G(d,p) calculations) are listed in Table 1. We can see differences in average time among these substituents are small. Figure 2 plots the average whole time versus Hammett  $\sigma_p$  values.<sup>17</sup> These results indicate only a weak correlation between  $\pi$ -donating ability of substituents and velocities. However, removing X = H from these plots leads to better, although still not strong, correlations (Figure 3), i.e., it appears that most any substituent is better than a hydrogen in terms of promoting a velocity increase. This observation prompted us to explore the origins of rate acceleration in more depth. Also, the increased H migration velocity with stronger donors is consistent with lower overall free energy barriers for these systems,<sup>1b</sup> but opposite to what one would expect based on the electrostatic drag concept; i.e., stronger donors would lead to stronger H– $\pi$  interactions, which would be expected to slow hydrogen motion.

Table 1. Results of the Hammett  $\sigma_p$  values of each substituent at para position of phenyl and average whole time for hydrogen migration in Figure 1.

X	TSS	Hammett $\sigma_p$ values	Average whole time(fs)	Total trajectories	TSS barrier(kcal/mol)
N(CH <sub>3</sub> ) <sub>2</sub>	<b>TS-N(CH<sub>3</sub>)<sub>2</sub></b>	-0.83	60.8	104	26.4
OCH <sub>3</sub>	<b>TS-OCH<sub>3</sub></b>	-0.27	63.6	122	26.8
H	<b>TS-H</b>	0	66.6	117	27.6
CF <sub>3</sub>	<b>TS-CF<sub>3</sub></b>	0.54	66.3	143	33.5
CN	<b>TS-CN</b>	0.66	66.2	131	32.9
NO <sub>2</sub>	<b>TS-NO<sub>2</sub></b>	0.78	65.2	109	30.9

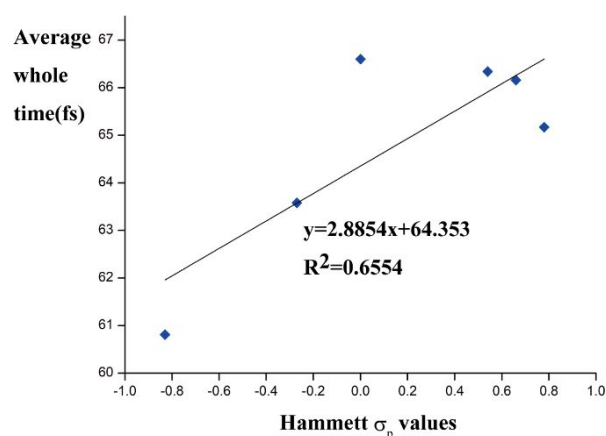


Figure 2. Correlation between Hammett  $\sigma_p$  values and average whole time.

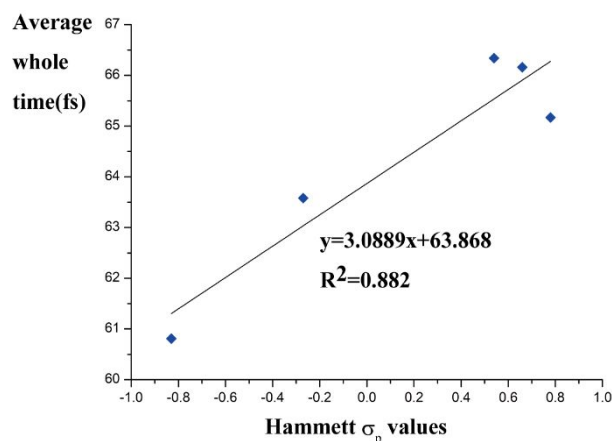


Figure 3. Correlation between Hammett  $\sigma_p$  values and average whole time removing X = H.

We postulated that the observations above might be pointing to an effect of dispersion, i.e., increased surface area leads to longer contact times between the migrating hydrogen and the  $\pi$ -surface of the aryl group. To test this hypothesis, we repeated our calculations for X = N(CH<sub>3</sub>)<sub>2</sub>, H and NO<sub>2</sub> with levels of theory that are better at capturing dispersion effects.<sup>13,14</sup> Results from trajectories obtained with B3LYP-D3 and M06-2X are shown in Tables 2 and 3 and do not suggest a strong effect of dispersion on relative velocities. Again, while H-migration for systems with X = N(CH<sub>3</sub>)<sub>2</sub> is predicted to be faster than with X = NO<sub>2</sub> in each case, the predicted velocities for X = H are more variable.

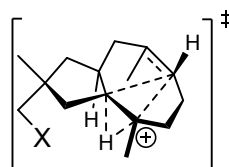
Table 2. Results from Dynamics Trajectories Initiated from **TS-NMe<sub>2</sub>**, **TS-H** and **TS-NO<sub>2</sub>** (B3LYP-D3/6-31+G(d,p))

X (B3LYP-D3)	TSS	Average whole time(fs)	Total trajectories
N(CH <sub>3</sub> ) <sub>2</sub>	<b>TS-N(CH<sub>3</sub>)<sub>2</sub></b>	50.8	104
H	<b>TS-H</b>	60.8	119
NO <sub>2</sub>	<b>TS-NO<sub>2</sub></b>	63.9	103

Table 3. Results from Dynamics Trajectories Initiated from **TS-NMe<sub>2</sub>**, **TS-H** and **TS-NO<sub>2</sub>** (M06-2X/6-31+G(d,p))

X (M06-2X)	TSS	Average whole time(fs)	Total trajectories
N(CH <sub>3</sub> ) <sub>2</sub>	<b>TS-N(CH<sub>3</sub>)<sub>2</sub></b>	81.1	103
H	<b>TS-H</b>	78.3	102
NO <sub>2</sub>	<b>TS-NO<sub>2</sub></b>	89.6	108

Keeping in mind the argument that direct electrostatic interactions with substituents are generally more important than  $\pi$ -polarization (at least for  $\pi$ - $\pi$  stacking),<sup>18</sup> we expanded our study to include systems without benzene rings (Figure 4). The results of trajectory simulations for these systems are listed in Table 4 (and plotted in Figure 5), which also shows CHelpG charges for the atoms that are closest to the migrating H for each TSS (Table 5). The results in Table 4 and Figure 5 indicate that stronger electrostatic interactions do lead to slower hydrogen migration, consistent with the electrostatic drag concept, although the correlation is again rough.



X = H, furan, CH=CH<sub>2</sub>, NO, N(CH<sub>3</sub>)<sub>2</sub>, F,  
NO<sub>2</sub>, OCH<sub>3</sub>, SCH<sub>3</sub>, CH=O, CN

Figure 4. Non-benzenoid groups used to explore hydrogen migration process.

Table 4. Results of the CHelpG charges for each substituent and average whole time for hydrogen migration in Figure 4.

X	TSS	CHelpG charges <sup>a</sup>	Average whole time (fs)	Total trajectories
CHO	<b>TS<sub>CHO</sub></b>	-0.545	98.6	86
NO <sub>2</sub>	<b>TS<sub>NO2</sub></b>	-0.491	84.3	85
CN	<b>TS<sub>CN</sub></b>	-0.470	99.0	74
OCH <sub>3</sub>	<b>TS<sub>OCH3</sub></b>	-0.307	88.3	92
F	<b>TS<sub>F</sub></b>	-0.297	71.3	89
SCH <sub>3</sub>	<b>TS<sub>SCH3</sub></b>	-0.189	93.5	82
CH=CH <sub>2</sub>	<b>TS<sub>CH=CH2</sub></b>	-0.159	66.3	119
NO	<b>TS<sub>NO</sub></b>	-0.121	69.1	111
H	<b>TS<sub>H</sub></b>	0.049	62.4	105
NMe <sub>2</sub>	<b>TS<sub>NMe2</sub></b>	0.066	70.0	93
Furan	<b>TS<sub>Furan</sub></b>	0.100	66.2	90

<sup>a</sup> For the transition states with two atoms that are nearly close to the migrating H shown in Table 5, we average the CHelpG charges of the two atoms.

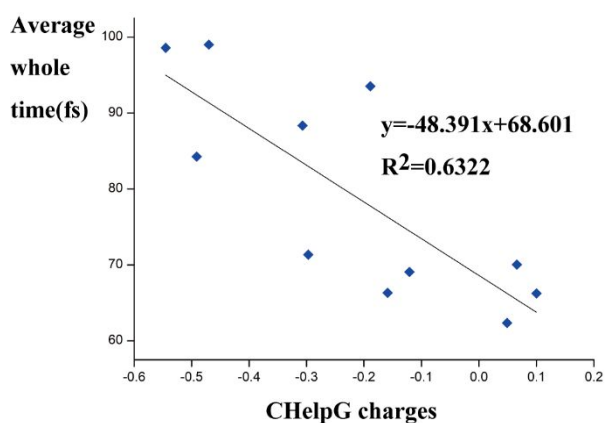
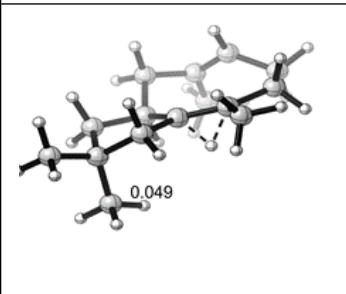
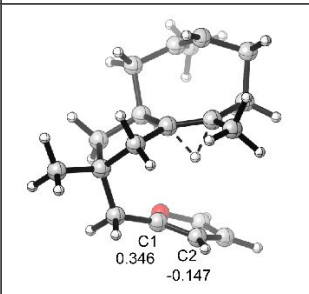
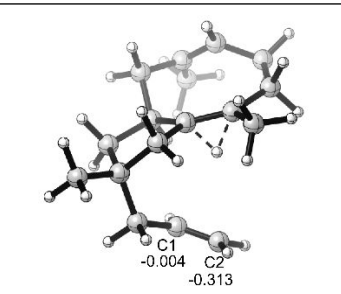
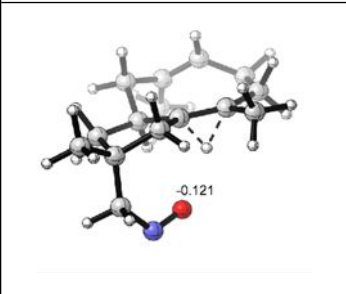
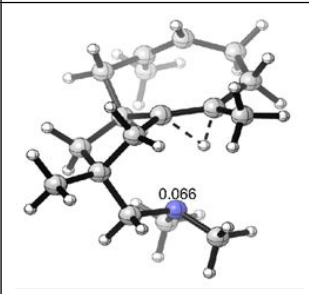
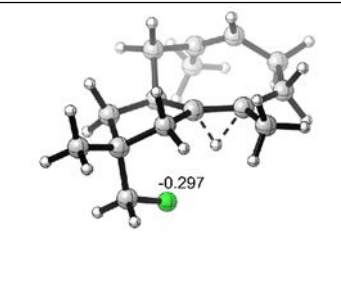
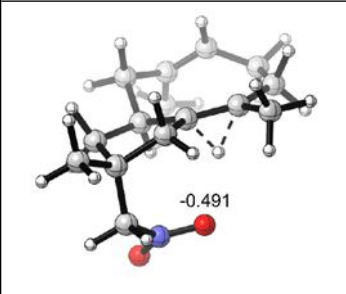
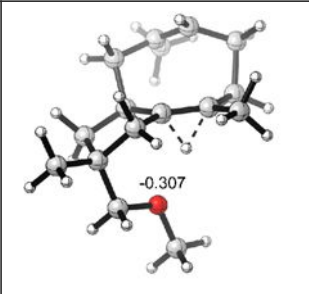
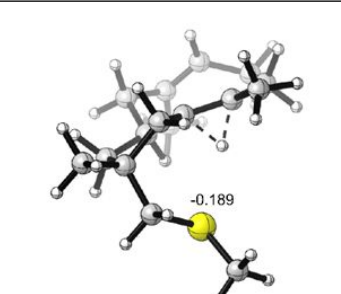
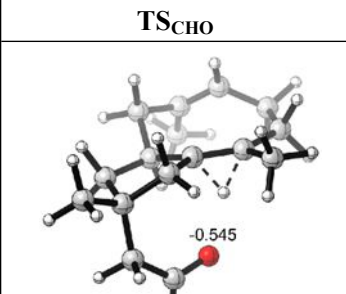
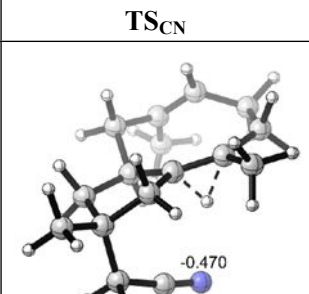


Figure 5. Correlation between CHelpG charges and the average whole time.

Table 5. Optimized structures of hydrogen migration TSSs with non-aromatic groups, along with CHelpG charges.

<b>TS<sub>H</sub></b>	<b>TS<sub>Furan</sub></b>	<b>TS<sub>CH=CH<sub>2</sub></sub></b>
		
<b>TS<sub>NO</sub></b>	<b>TS<sub>NMe2</sub></b>	<b>TS<sub>F</sub></b>
		
<b>TS<sub>NO2</sub></b>	<b>TS<sub>OCH3</sub></b>	<b>TS<sub>SCH3</sub></b>
		
<b>TS<sub>CHO</sub></b>	<b>TS<sub>CN</sub></b>	
		



How do these results connect to entropy? To crudely estimate entropic contributions, we carried out single point frequency calculations along IRCs; two examples, for the systems with most negative (CHO) and most positive (furan) CHelpG charges, are shown in Figure 6. For both cases, the entropy improves in the region of the TSS because the hydrogen is less constrained than in the reactant or product. However, the improvement is less for system with the more negatively charged neighboring group (CHO), in line with stronger H•••X interactions. A similar scenario is observed when using VTSs (Figure 7). Note that the charges vary little along the IRCs (Figure 6), consistent with the effect being primarily electrostatic in nature.

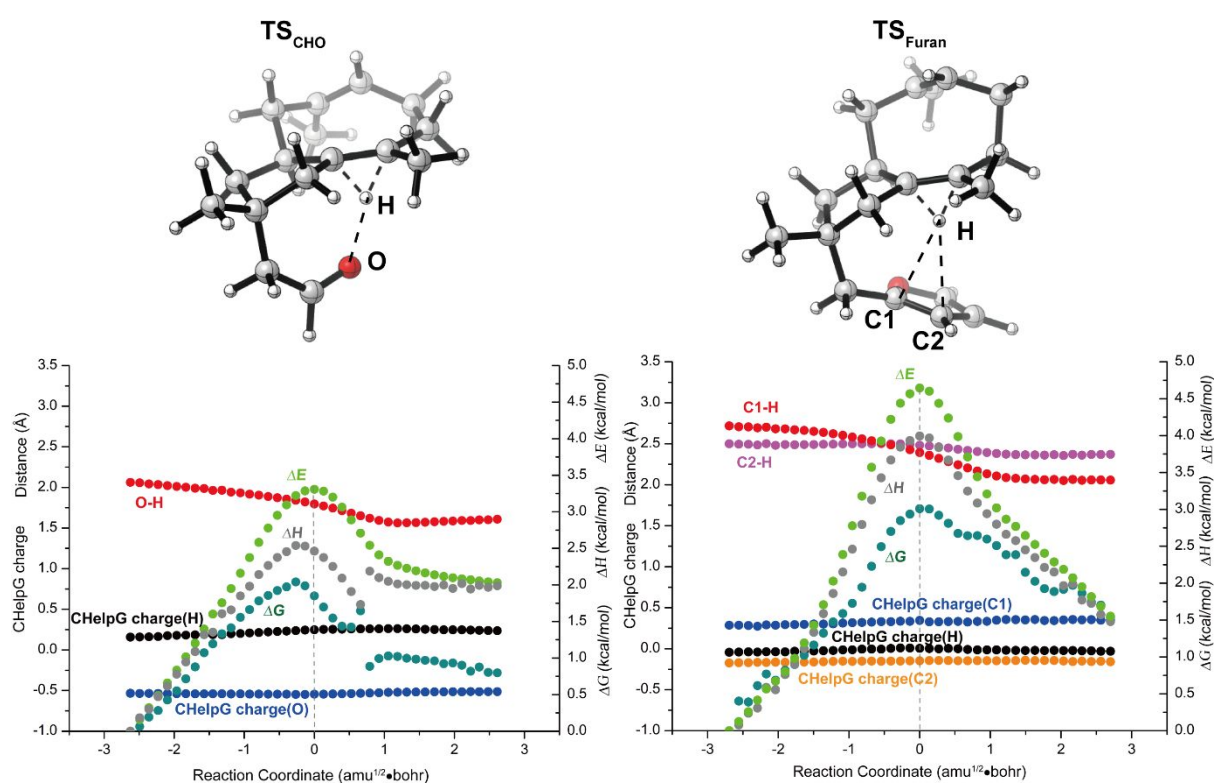


Figure 6. Gibbs free energy ( $\Delta G$ ), electronic energy ( $\Delta E$ ), enthalpy ( $\Delta H$ ), CHelpG charges, and calculated bond distances along the IRCs for  $\text{TS}_{\text{CHO}}$  and  $\text{TS}_{\text{Furan}}$ . Free energy barriers for the CHO- and furan-containing systems are predicted to be 24.6 and 15.3 kcal/mol, respectively.

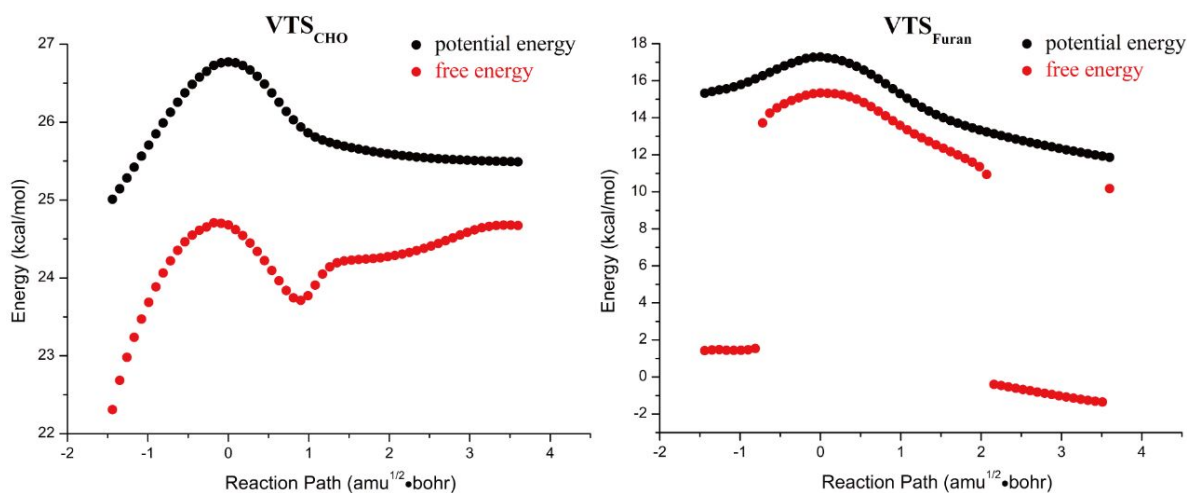


Figure 7. Generalized standard-state activation free energy and potential energy along the reaction paths for  $VTS_{CHO}$  and  $VTS_{Furan}$ . The discontinuities in the righthand plot persist even when employing the RODS algorithm (see SI), but do not impact our conclusions.

#### 4. Conclusions

The concept of electrostatic drag was explored in the context of a model hydrogen migration reaction. Hydrogen migration velocity was shown to vary with the strength of electrostatic interactions between the hydrogen and neighboring groups. Enthalpically favorable electrostatic interactions led to lower free energy barriers (Figure 6) but also to entropic penalties that are correlated to slower hydrogen motion. In effect, we have shown that one can characterize a *local entropy effect* on particular molecular substructures whose motion may or may not be synchronous with motions of other substructures during a reaction. Since electrostatic drag modulates substructure velocity it can, in principle, be used to modulate synchronicity,<sup>19</sup> which has implications for modulating selectivity – a concept we are currently exploring. While enthalpy/entropy compensation is not a new concept, the relationship to electrostatic drag demonstrated here opens the door to both rationalizing previous experimental results and designing new reactions that use electrostatic drag to advantage.

**Associated Content****Supporting Information**

Additional details on dynamics calculations, coordinates and energies for computed structures.

**Author Information****Corresponding Authors**

\*djtantillo@ucdavis.edu

**Notes**

The authors declare no competing financial interest.

**Acknowledgments**

Support from the National Science Foundation (CHE-1856416 and supercomputing resources from the XSEDE program via CHE-030089) and the Overseas Research and Study Program for Doctoral Students in Shandong Province is gratefully acknowledged.

**Reference**

- 1 (a) P. Gutta and D. J. Tantillo, *J. Am. Chem. Soc.*, 2006, **128**, 6172–6179; (b) M. W. Lodewyk, D. Willenbring and D. J. Tantillo, *Org. Biomol. Chem.*, 2014, **12**, 887–894; (c) L. Zu, M. Xu, M. W. Lodewyk, D. E. Cane, R. J. Peters and D. J. Tantillo, *J. Am. Chem. Soc.*, 2012, **134**, 11369–11371.
- 2 (a) R. J. Buenker, S. D. Peyerimhoff, L. C. Allen and J. L. Whitten, *J. Chem. Phys.*, 1966, **45**, 2835–2847; (b) I. Fernandez, F. P. Cossio and M. A. Sierra, *Chem. Rev.*, 2009, **109**, 6687–6711; (c) O. Gutierrez and D. J. Tantillo, *J. Org. Chem.*, 2012, **77**, 8845–8850; (d) R. Hoffmann and J. E. Williams, Jr., *Helv. Chim. Acta*, 1972, **55**, 67–75; (e) M. Reetz, *Tetrahedron*, 1973, **29**, 2189–2194; (f) M. T. Reetz, *Angew. Chem., Int. Ed.*, 1972, **11**, 129–130; (g) M. T. Reetz, *Angew. Chem., Int. Ed.*, 1972, **11**, 130–131; (h) M. T. Reetz, *Adv. Organomet. Chem.*, 1977, **16**, 33–65.
- 3 (a) D. A. Dougherty, *J. Nutr.*, 2007, **137**, 1504S–1508S; (b) D. A. Dougherty, *Acc. Chem. Res.*, 2013, **46**, 885–893; (c) J. P. Gallivan and D. A. Dougherty, *Proc. Natl. Acad. Sci. U.S.A.*, 1999, **96**, 9459–9464; (d) J. C. Ma and D. A. Dougherty, *Chem. Rev.*, 1997, **97**, 1303–1324; (e) S. Mecozzi, A. P. West and D. A. Dougherty, *Proc. Natl. Acad. Sci. U.S.A.*, 1996, **93**, 10566–10571.
- 4 S. R. Hare, R. P. Pemberton and D. J. Tantillo, *J. Am. Chem. Soc.*, 2017, **139**, 7485–7493.
- 5 (a) E. Grunwald and C. Steel, *J. Am. Chem. Soc.*, 1995, **117**, 5687–5692; (b) E. A. Meyer, R. K. Castellano and F. Diederich, *Angew. Chem., Int. Ed.*, 2003, **42**, 1210–1250; (c) K. N. Houk, A. G. Leach, S. P. Kim and X. Zhang, *Angew. Chem., Int. Ed.*, 2003, **42**, 4872–4897.
- 6 M. J. Frisch, G. W. Trucks, H. B. Schlegel, G. E. Scuseria, M. A. Robb, J. R. Cheeseman, G. Scalmani, V. Barone, B. Mennucci, G. A. Petersson, H. Nakatsuji, M. Caricato, X. Li, H. P. Hratchian, A. F. Izmaylov, J. Bloino, G. Zheng, J. L. Sonnenberg, M. Hada, M. Ehara, K. Toyota, R. Fukuda, J. Hasegawa, M. Ishida, T. Nakajima, Y. Honda, O. Kitao, H. Nakai, T. Vreven, J. A. Montgomery Jr., J. E. Peralta, F. Ogliaro, M. Bearpark, J. J. Heyd, E. Brothers, K. N. Kudin, V. N. Staroverov, T. Keith, R. Kobayashi, J. Normand, K. Raghavachari, A. Rendell, J. C. Burant, S. S. Iyengar, J. Tomasi, M. Cossi, N. Rega, J. M. Millam, M. Klene, J. E. Knox, J. B. Cross, V. Bakken, C. Adamo, J. Jaramillo, R. Gomperts, R. E. Stratmann, O. Yazyev, A. J. Austin, R. Cammi, C. Pomelli, J. W. Ochterski, R. L. Martin, K. Morokuma, V. G. Zakrzewski, G. A. Voth, P. Salvador, J. J. Dannenberg, S. Dapprich, A. D. Daniels, O. Farkas, J. B. Foresman, J. V. Ortiz, J. Cioslowski and D. J. Fox, *Gaussian 09, Revision D.01*; Gaussian, Inc.: Wallingford, CT, 2009.

- 7 (a) A. D. Becke, *Phys. Rev. A: At., Mol., Opt. Phys.*, 1988, **38**, 3098–3100; (b) A. D. Becke, *J. Chem. Phys.*, 1993, **98**, 1372–1377; (c) C. Lee, W. Yang and R. G. Parr, *Phys. Rev. B: Condens. Matter Mater.*, 1988, **37**, 785–789; (d) B. Miehlich, A. Savin, H. Stoll and H. Preuss, *Chem. Phys. Lett.*, 1989, **157**, 200–206; (e) R. Ditchfield, W. J. Hehre and J. A. Pople, *J. Chem. Phys.*, 1971, **54**, 724–728.
- 8 J. Zheng, J. L. Bao, S. Zhang, J. C. Corchado, R. Meana-Pañeda, Y.-Y. Chuang, E. L. Coitiño, B. A. Ellingson and D. G. Truhlar. Gaussrate 17, University of Minnesota, Minneapolis, MN, 2017.
- 9 J. Zheng, J. L. Bao, R. Meana-Pañeda, S. Zhang, B. J. Lynch, J. C. Corchado, Y.-Y. Chuang, P. L. Fast, W.-P. Hu, Y.-P. Liu, G. C. Lynch, K. A. Nguyen, C. F. Jackels, A. Fernandez Ramos, B. A. Ellingson, V. S. Melissas, J. Villà, I. Rossi, E. L. Coitiño, J. Pu, T. V. Albu, A. Ratkiewicz, R. Steckler, B. C. Garrett, A. D. Isaacson and D. G. Truhlar. Polyrate 17, University of Minnesota, Minneapolis, 2017.
- 10 (a) K. Fukui, *Acc. Chem. Res.*, 1981, **14**, 363–368; (b) L. W. Chung, W. M. C. Sameera, R. Ramozzi, A. J. Page, M. Hatanaka, G. P. Petrova, T. V. Harris, X. Li, Z. Ke, F. Liu, H.-B. Li, L. Ding and K. Morokuma, *Chem. Rev.*, 2015, **115**, 5678–5796; (c) S. Maeda, Y. Harabuchi, Y. Ono, T. Taketsugu and K. Morokuma, *Int. J. Quantum Chem.*, 2015, **115**, 258–269.
- 11 B. R. Ussing, C. Hang and D. A. Singleton, *J. Am. Chem. Soc.*, 2006, **128**, 7594–7607.
- 12 (a) U. Lourderaj, K. Park and W. L. Hase, *Int. Rev. Phys. Chem.*, 2008, **27**, 361–403; (b) G. H. Peslherbe, H. Wang and W. L. Hase, *Adv. Chem. Phys.*, 1999, **105**, 171–201.
- 13 (a) S. Grimme, J. Antony, S. Ehrlich and H. Krieg, *J. Chem. Phys.*, 2010, **132**, 154104; (b) S. Grimme, S. Ehrlich and L. Goerigk, *J. Comput. Chem.*, 2011, **32**, 1456–1465. (c) Y. Zhao and D. G. Truhlar, *Theor. Chem. Acc.*, 2008, **120**, 215–241; (d) Y. Zhao and D. G. Truhlar, *Acc. Chem. Res.*, 2008, **41**, 157–167.
- 14 (a) D. H. Aue, *WIREs Comp. Molec. Sci.*, 2011, **1**, 487–508. (b) D. J. Tantillo, *Angew. Chem. Int. Ed.*, 2017, **56**, 10040–10045.
- 15 C. Y. Legault, *CYLView, 1.0b*, Université de Sherbrooke: Québec, Montreal, Canada, 2009, <http://www.cylview.org>.
- 16 (a) C. M. Breneman and K. B. Wiberg, *J. Comput. Chem.*, 1990, **11**, 361–373; (b) G. S. Maciel and E. Garcia, *Chem. Phys. Lett.*, 2005, **409**, 29–33; (c) K. B. Wiberg and P. R. Rablen, *J. Comput. Chem.*, 1993, **14**, 1504–1518.
- 17 (a) S. L. Broman, M. Jevric and M. B. Nielsen, *Chem. –Eur. J.*, 2013, **19**, 9542–9548; (b) K. C. Gross, P. G. Seybold, Z. Peralta-Inga, J. S. Murray and P. Politzer, *J. Org. Chem.*, 2001, **66**, 6919–6925; (c) C. Hansch, A. Leo and R. Taft, *Chem. Rev.*, 1991, **91**, 165–195.
- 18 (a) R. M. Parrish and C. D. Sherrill, *J. Am. Chem. Soc.*, 2014, **136**, 17386–17389; (b) S. E. Wheeler, *J. Am. Chem. Soc.*, 2011, **133**, 10262–10274; (c) R. J. Burns, I. K. Mati, K. B. Muchowska, C. Adam and S. L. Cockroft, *Angew. Chem., Int. Ed.*, 2020, **59**, 16717–16724.
- 19 (a) D. J. Tantillo, *J. Phys. Org. Chem.*, 2008, **21**, 561–570; (b) A. Williams, *Concerted Organic and Bio-organic Mechanisms*, CRC Press, 2000; (c) B. A. Hess, *J. Am. Chem. Soc.*, 2002, **124**, 10286–10287; (d) M. J. Dewar and A. B. Pierini, *J. Am. Chem. Soc.*, 1984, **106**, 203–208; (e) K. N. Houk, J. Gonzalez and Y. Li, *Acc. Chem. Res.*, 1995, **28**, 81–90.